ORICPublications
www.oricpub.com

Online available since 2016/ October /29 at www.oricpub.com

Journal of Chemistry and Materials Research
Vol. 5 (5), 2016, 99–104

ISSN: 2381-3628
JCMR
Journal of Chemistry and Materials Research
www.oricpub.com/jcmr

Original Research

Temperature Dependence of High-Order Expanded Debye–Waller Factors and XAFS of Metallic Molybdenium

Nguyen Van Hung [1,*], Trinh Thi Hue [1], Nguyen Ba Duc [2], Dinh Quoc Vuong [3]

[1]*Department of Physics, Hanoi University of Science. 334 Nguyen Trai, Thanh Xuan, Hanoi, Vietnam.*

[2]*Department of Physics, Tan Trao University, Km6, Trung Mon, Yen Son, Tuyen Quang, Vietnam.*

[3]*Quang Ninh Education & Training Department. Nguyen Van Cu, Ha Long, Quang Ninh, Vietnam.*

Received 25 September 2016; received in revised form 05 October 2016; accepted 10 October 2016

Abstract

Temperature dependence of high-order expanded Debye-Waller factors and X-ray absorption fine structure (XAFS) of Mo, a bcc crystal, has been studied based on the anharmonic correlated Debye model. The many-body effects are taken into account in the present one-dimensional model based on the anharmonic effective potential that includes interactions of absorber and backscatterer atoms with their first shell near neighbors, where Morse potential is assumed to describe the single-pair atomic interaction. Analytical expressions for the dispersion relation, correlated Debye frequency and temperature and four first temperature-dependent XAFS cumulants of bcc crystals have been derived using the many-body perturbation approach. The obtained cumulants have been applied to calculating XAFS spectra and their Fourier transform magnitudes. Numerical results for Mo are found to be in good agreement with experiment.

Keywords: Debye-Waller factor; Effective potential; Correlated Debye model; XAFS; Bcc crystals; Molybdenium.

1. Introduction

X-ray Absorption Fine Structure (XAFS) has developed into a powerful technique for providing information on the local atomic structure and thermal effects of substances [1–15]. The formalism for including anharmonic effects in XAFS is often based on the cumulant expansion approach [1] from which the expression for anharmonic XAFS has resulted as

$$\chi(k) = F(k)\frac{e^{-2R/\lambda(k)}}{kR^2}\mathrm{Im}\left\{e^{i\Phi(k)}\exp\left[2ikR + \sum_n \frac{(2ik)^n}{n!}\sigma(n)\right]\right\} \quad (1)$$

where $F(k)$ is the real atomic backscattering amplitude, k and λ are the wave number and mean free path of the photoelectron, respectively, Φ is net phase shift and $\sigma^{(n)}$ (n = 1, 2, 3, 4, …) are the cumulants describing the high-order expanded Debye-Waller factors (DWFs).

The cumulants contained in Eq. (1) are obtained due to the thermal average of the function exp(i2**k.r**) in which the asymmetric terms are expanded in a Taylor series about R = $\langle r \rangle$ with r being the instantaneous bond length between absorber and backscatterer atoms and the mean free path λ is defined based on the imaginary part of the complex photoelectron momentum $p = k + i/\lambda$.

Hence, the cumulants are very important for the accurate structural determinations (e.g., the coordination numbers and the atomic distances) from XAFS experiment, where the even cumulants contribute to the amplitude, the odd one to the phase of XAFS spectra and for small anharmonicities, it is sufficient to keep the third and fourth cumulant terms [2]. Then, if limiting to the fourth cumulant, the temperature T- and wave number k-dependent anharmonic contributions to the amplitude F_A and phase Φ_A of XAFS have the forms

$$F_A(k,T) = \exp\left(-\frac{2}{3}k^4\sigma^{(4)}(T)\right),$$
$$\Phi_A(k,T) = -\frac{4k\sigma^2(T)}{R}\left(1+\frac{R}{\lambda}\right) - \frac{4}{3}k^3\sigma^{(3)}(T). \quad (2)$$

Many efforts have been made to develop procedures for the calculation and analysis of XAFS cumulants. The classical

* Corresponding author. Tel.: +000 00000000; fax: +000 00000000.
E-mail address: hungnv@vnu.edu.vn *(**N.V. Hung**).*

theories are simpler and work well at high-temperatures [3–5], but they cannot be valid at low-temperatures due to zero-point vibration. The quantum methods [6–15] can work at all temperatures. The anharmonic effective single-particle (AESP) potential [2] provide some qualitative understanding of the anharmonic XAFS experiment but it does not give an accurate description of the situation because of ignoring correlated motion. The anharmonic correlated Einstein single-bond (SB) model [8], the full lattice dynamical (FLD) method [8] include the atomic correlation but they use the SB [8] and single-pair (SP) [9] potentials neglecting the contributions of the many-body effects. The anharmonic correlated Einstein model (ACEM) [10–14] includes the near neighbor contributions based on a small cluster but it considers the cumulants only up to the third order. The statistical moment method (SMM) [15] has the advantage by including the anharmonic effects in atomic vibration for semiconductors and compounds but it has not yet developed for the calculation and analysis of high-order expanded DWFs. In particular, there is still few methods for studying DWFs with high-order expansion and no theoretical result on XAFS for bcc crystals while their experimental results are available [16].

The purpose of this work is to study temperature dependence of high-order expanded DWFs of bcc crystals derived based on the anharmonic correlated Debye model (ACDM) [17] and their application to calculating XAFS Fourier transform magnitude (FTM) providing structural parameters of the material. In Section 2 the derivations of the analytical expressions have been presented firstly, for the anharmomic interatomic effective potential of bcc crystals based on the first shell near neighbor contribution approach (FSNNCA) and secondly, the analytical expressions of four first temperature-dependent XAFS cumulants of bcc crystals using the many-body perturbation approach (MBPA) [18], dispersion relation and the parameters of the derived anharmonic effective potential, where Morse potential is assumed to describe the single-pair atomic interaction. The obtained cumulants have been applied to calculating XAFS and their FTMs based on Eqs. (1) and (2). Numerical results for Mo (Section 3) are compared to experiment [16] which show good agreement and their advantage compared to those calculated using the SB and SP potentials.

2. Formalism

In order to include the anharmonic effects in XAFS, Hamiltonian of the system is written in the summation of the harmonic and anharmonic components, H_0 and H_a, respectively

$$H = H_0 + H_a,\ H_a = H_c + H_q \tag{3}$$

where the anharmonic component H_a contains the cubic H_c and quartic H_q terms including the anharmonic interatomic effective potential parameters of bcc crystals.

The anharmonic interatomic *effective potential* expanded up to the fourth order in the present theory for bcc crystals is expressed as a function of the displacement $x = r - r_0$ along the bond direction with r and r_0 being the instantaneous and equilibrium distances between absorber and backscatterer atoms, respectively.

$$V_{eff}(x) \approx \frac{1}{2}k_{eff}x^2 + k_{3eff}x^3 + k_{4eff}x^4 \tag{4}$$

where k_{eff} is the effective local force constant, k_{3eff} and k_{4eff} are the anharmonic parameters giving an asymmetry of the anharmonic effective potential.

For bcc crystals each atom is bonded to 8 near neighbors. Then the effective potential Eq. (4) defined based on the FSNNCA has the form

$$V_{eff}(x) = V(x) + 2V\left(-\frac{x}{2}\right) + 6V\left(\frac{x}{6}\right) + 6V\left(-\frac{x}{6}\right) \tag{5}$$

which is the sum over not only the term V(x) describing the pair-interaction between absorber and backscatterer atoms but also the other terms describing the projections of their pair-interactions with 14 first shell near neighbors of bcc crystals along the bond direction excluding the absorber and backscatterer themselves whose contributions are already described by V(x).

Applying Morse potential expanded up to the fourth order as:

$$\begin{aligned} V(x) &= D\left(e^{-2\alpha x} - 2e^{-\alpha x}\right) \\ &\approx D\left(-1 + \alpha^2x^2 - \alpha^3x^3 + \frac{7}{12}\alpha^4x^4\right) \end{aligned} \tag{6}$$

to each term of Eq. (5) and comparing the result to Eq. (4), we obtain the values of $k_{eff}, k_{3eff}, k_{4eff}$ for bcc crystals in terms of Morse potential parameters

$$k_{eff} = \frac{11}{3}D\alpha^2,\ k_{3eff} = -\frac{3}{4}D\alpha^3,\ k_{4eff} = \frac{1715}{2592}D\alpha^4 \tag{7}$$

where α describes the width of the potential and D is dissociation energy.

Hence, the anharmonic effective potential for bcc crystals of Eq. (5) has resulted as:

$$V_{eff}(x) \approx \frac{11}{6}D\alpha^2x^2 - \frac{3}{4}D\alpha^3x^3 + \frac{1715}{2592}D\alpha^4x^4 \tag{8}$$

which is different from the SB and SP potentials denoted for both by SPP because they are the same containing only the term V(x) describing the pair-interaction between absorber and backscatterer atoms. From Eq. (6) the SPP has the following form:

$$V_{SP}(x) = V(x) \approx D\alpha^2x^2 - D\alpha^3x^3 + \frac{7}{12}D\alpha^4x^4 \tag{9}$$

Note that the above mentioned lattice contributions based on the FSNNCA, to the oscillation between absorber and backscatterer atoms described by the projections of their pair-interactions with 14 first shell near neighbors along the bond direction, make it possible to take into account the many–body effects in the present one-dimensional model for bcc crystals.

Derivation of the present ACDM for bcc crystals using the MBPA [18] is based on the dualism of an elementary particle in quantum theory, i.e., its corpuscular and wave property.

Then, we can describe the system in Debye model involving all different frequencies up to the Debye frequency as a system consisting of many bodies, i.e., of many phonons each of which corresponds to a wave having frequency $\omega(q)$ and wave number q varied in the first Brillouin zone (BZ).

For the derivation, the displacement $u_n's$ in the parameter x in terms of the displacement of nth atom u_n of the one dimensional chain described by:

$$x_n = u_{n+1} - u_n \tag{10}$$

is related to the phonon displacement operators A_q [19] in the form

$$u_n = \sqrt{\frac{\hbar}{2NM}} \sum_q \frac{e^{iqan}}{\sqrt{\omega(q)}} A_q \,,\; A_q = A_{-q}^{+},\; \left[A_q, A_{q'}\right] = 0 \tag{11}$$

to be given by

$$x_n = \sum_q e^{iqan} f(q) A_q, \quad f(q) = \sqrt{\frac{\hbar}{2NM\omega(q)}} \left(e^{iqa} - 1\right) \tag{12}$$

where N is atomic number, M is the mass of composite atoms and a is lattice constant.

The frequency $\omega(q)$ contained in Eq. (12) and then in all cumulant expressions derived for the vibration between absorber and backscatterer atoms in XAFS process describes the dispersion relation. Using the local force constant of the first equation of Eqs. (7), it has resulted as

$$\omega(q) = 2\alpha \sqrt{\frac{11D}{3M}} \left|\sin\left(\frac{qa}{2}\right)\right|, \quad |q| \le \frac{\pi}{a} \tag{13}$$

At the bounds of the first BZ of the linear chain, $q = \pm\pi/a$, the frequency has maximum so that from Eq. (13) we obtain the correlated Debye frequency ω_D and temperature θ_D for bcc crystals in the form

$$\omega_D = 2\alpha \sqrt{\frac{11D}{3M}}, \quad \theta_D = \frac{\hbar\omega_D}{k_B} \tag{14}$$

where k_B is Boltzmann constant.

Using the above results in the MBPA [18], we have derived the analytical expressions for XAFS DWFs presented in terms of cumulant expansion up to the fourth order for bcc crystals.

The first cumulant describing the net thermal expansion or disorder in XAFS theory has resulted as

$$\sigma^{(1)}(T) = \langle x \rangle = \sigma_0^{(1)} \int_0^{\pi/a} \omega(q) \frac{1+Z(q)}{1-Z(q)} dq = \frac{\sigma_0^{(1)}}{\sigma_0^2} \sigma^2 \,,$$
$$\sigma_0^{(1)} = \frac{81a\hbar}{484\pi D\alpha}, \; Z(q) = \exp(\beta\hbar\omega(q)), \; \beta = 1/k_B T. \tag{15}$$

Here, σ^2 is second cumulant describing the mean square relative displacement (MSRD) and has the following form

$$\sigma^2(T) = \left\langle x^2 \right\rangle = \sigma_0^2 \int_0^{\pi/a} \omega(q) \frac{1+z(q)}{1-z(q)} dq \,,$$
$$\sigma_0^2 = \frac{3\hbar a}{22\pi D\alpha^2}. \tag{16}$$

The third cumulant is the mean cubic relative displacement (MCRD) describing the asymmetry of the pair distribution function in XAFS theory and has resulted as

$$\sigma^{(3)}(T) \cong \left\langle x^3 \right\rangle - 3\left\langle x^2 \right\rangle \langle x \rangle =$$
$$\sigma_0^{(3)} \int_0^{\pi/a} dq_1 \int_{-\pi/d}^{\pi/a - q_1} dq_2 \frac{\omega(q_1)\omega(q_2)\omega(q_1+q_2)}{\omega(q_1)+\omega(q_2)+\omega(q_1+q_2)}$$
$$\times \left\{ 1 + 6\frac{\omega(q_1)+\omega(q_2)}{\omega(q_1)+\omega(q_2)-\omega(q_1+q_2)} \frac{e^{\beta\hbar[\omega(q_1)+\omega(q_2)]} - e^{\beta\hbar\omega(q_1+q_2)}}{\left(e^{\beta\hbar\omega(q_1)}-1\right)\left(e^{\beta\hbar\omega(q_2)}-1\right)\left(e^{\beta\hbar\omega(q_1+q_2)}-1\right)} \right\}, \tag{17}$$
$$\sigma_0^{(3)} = \frac{114\times10^{-4}\hbar^2 a^2}{\pi^2 D^2 \alpha^3}.$$

The fourth cumulant describing the anharmonic contribution to XAFS amplitude is given by:

$$\sigma^{(4)}(T) \cong \left\langle x^4 \right\rangle - 3\left\langle x^2 \right\rangle^2 =$$
$$\sigma_0^{(4)} \int_0^{\pi/a} dq_1 \int_0^{\pi/a - q_1} dq_2 \int_{-\pi/a}^{\pi/a-(q_1+q_2)} dq_3 \frac{\omega(q_1)\omega(q_2)\omega(q_3)\omega(q_4)}{\omega(q_1)+\omega(q_2)+\omega(q_3)+\omega(q_4)}$$
$$\times \left\{ 1 + 8\frac{Z(q_1)Z(q_2)Z(q_3)-Z(q_4)}{(Z(q_1)-1)(Z(q_2)-1)(Z(q_3)-1)(Z(q_4)-1)} \times \frac{\omega(q_1)+\omega(q_2)+\omega(q_3)}{\omega(q_1)+\omega(q_2)+\omega(q_3)-\omega(q_4)} \right.$$
$$\left. + 6\frac{Z(q_1)Z(q_2)-Z(q_3)Z(q_4)}{(Z(q_1)-1)(Z(q_2)-1)(Z(q_3)-1)(Z(q_4)-1)} \times \frac{\omega(q_3)+\omega(q_4)}{\omega(q_1)+\omega(q_2)-\omega(q_3)-\omega(q_4)} \right\}, \tag{18}$$
$$\sigma_0^{(4)} = \frac{165\times10^{-4}\hbar^3 a^3}{2\pi^3 D^3 \alpha^4}, \; q_4 = -(q_1+q_2+q_3).$$

Note that in the above expressions for the cumulants of bcc crystals, $\sigma_0^{(1)}, \sigma_0^2, \sigma_0^{(3)}, \sigma_0^{(4)}$ are zero-point energy contributions to the first, second, third and fourth cumulant, respectively, and these cumulant expressions have been obtained for the case of large atomic number N, when the summation over q is replaced by the corresponding integral in the first BZ.

3. Numerical results and discussions

Now the expressions derived in the previous section are applied to numerical calculations for Mo using its Morse potential

Table 1 Debye frequency ω_D and temperature θ_D of Mo calculated using the present theory compared to the experimental values (Expt.) [16] and to those calculated using the SPP parameters.

ω_D (10^{13}Hz)			θ_D (K)		
Present	Expt. [16]	SPP	Present	Expt. [16]	SPP
5.175	5.271	3.822	395.3	374.5±17	291.95

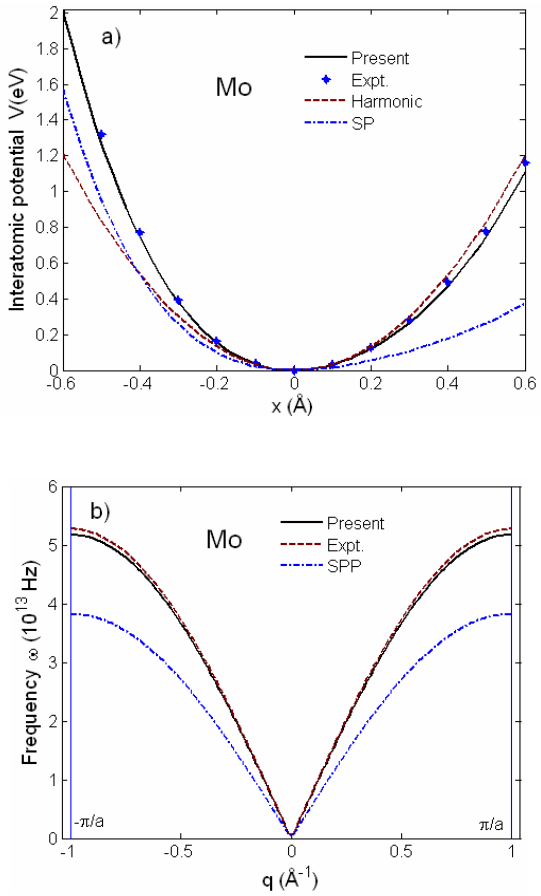

Fig. 1. a) Present anharmonic effective potentials $V_{eff}(x)$ and b) dispersion relation $\omega_{(q)}$ of Mo calculated using the present theory compared to experiment (Expt.) [16] and to those calculated using the SPP parameters.

π/a (Fig. 1b) for Mo is equal to its Debye frequency from which the Debye temperature has been calculated and written in Table 1. It is found to be in good agreement with experiment [16] and different from the one calculated using the SPP parameters.

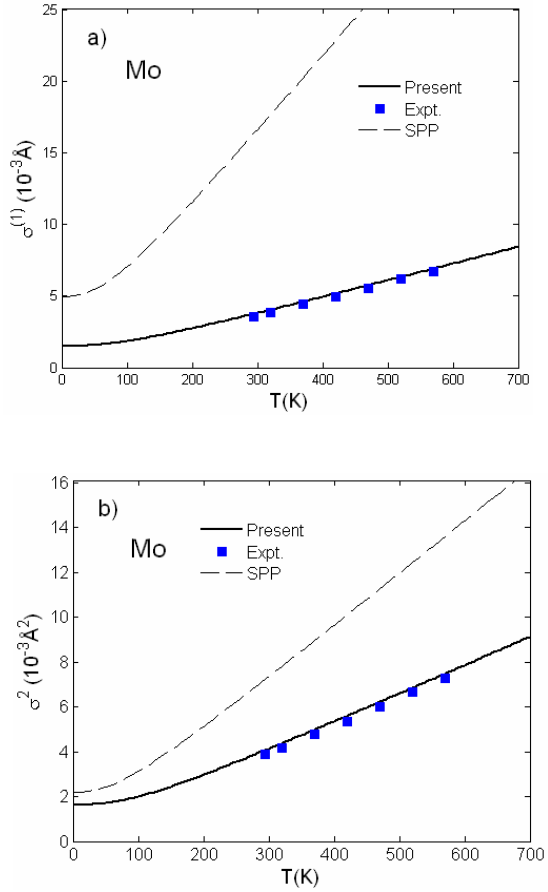

Fig. 2. Temperature dependence of a) first cumulant $\sigma^{(1)}$(T) and b) second cumulant σ^2(T) of Mo calculated using the present theory compared to the experimental values [16] and to those calculated using the SPP parameters.

parameters [20] D = 0.8032 eV, α = 1.5079 Å^{-1}. Table 1 shows good agreement of Debye frequency ω_D and temperature θ_D of Mo calculated using the present theory with the experimental values (Expt.) [16] and their significant difference from those calculated using the SPP parameters.

Fig. 1 illustrates good agreement of a) present anharmonic interatomic effective potential $V_{eff}(x)$ and b) dispersion relation $\omega(q)$ of Mo calculated using the present theory with experiment (Expt.) [16] and their significant difference from those calculated using the SPP parameters. This anharmonic interatomic effective potential is asymmetric due to the anharmonic contributions. The maximal value of frequency at

Figs. 2a and 2b, Figs. 3a and 3b illustrate good agreement of temperature-dependent first $\sigma^{(1)}$(T), second σ^2(T), third $\sigma^{(3)}$(T), and fourth $\sigma^{(4)}$(T) cumulants, respectively, of Mo calculated using the present theory with the experimental values [16] and their significant difference from those calculated using the SPP parameters presented here for $\sigma^{(1)}$(T) and σ^2(T) as examples. Such significant discrepancies can be attributed to neglecting the many-body effects in the SPP. The cumulant ratio $\sigma^{(1)}\sigma^2/\sigma^{(3)}$ (Fig. 4) also approaches the constant value at high-temperatures as for the ACEM [10]. This shows that above Debye temperature (θ_D = 395.30 K for Mo, Table 1) the classical limit is applicable for the present ACDM.

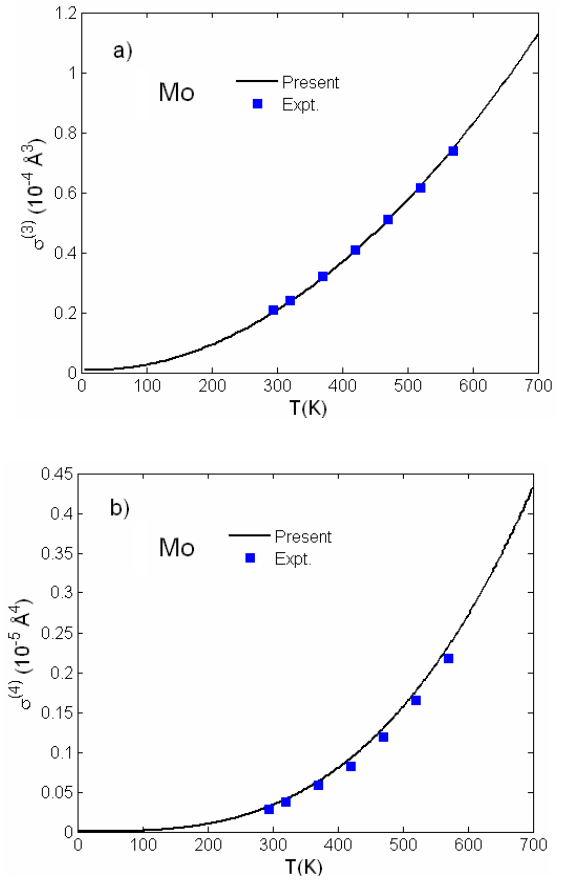

Fig. 3. Temperature dependence of a) third cumulant $\sigma^{(3)}$(T) and b) fourth cumulant $\sigma^{(4)}$(T) of Mo calculated using the present theory compared to the experimental values [16].

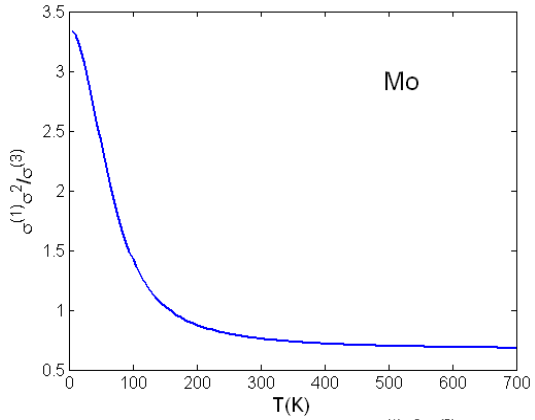

Fig. 4. Temperature dependence of cumulant ratio $\sigma^{(1)}\sigma^2/\sigma^{(3)}$ of Mo calculated using the present theory.

Fig. 5 illustrates good agreement of XAFS FTMs of Mo at 293 K and 573 K for the first shell calculated using Eqs. (1) and (2) and the obtained cumulants with the experimental results [16]. They are shifted when the temperature changes from 293 K to 573 K due to the anharmonic effects caused by the temperature dependence.

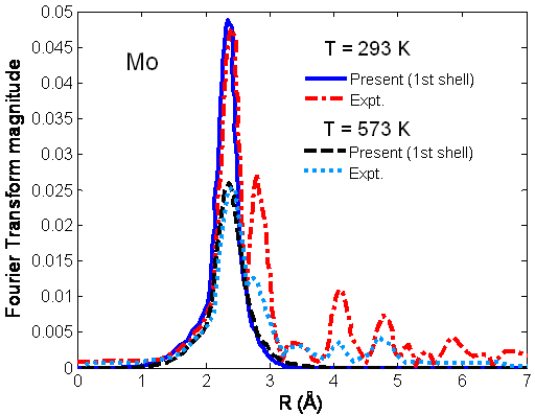

Fig. 5. XAFS FTMs for the first shell at 293 K and 573 K of Mo calculated using the present theory compared to experiment [16]

Based on the above obtained temperature-dependent cumulants agreeing well with experiment [16], the thermodynamic properties and anharmonic effects in XAFS of Mo can be in detail valuated. Here the first cumulant describes the net thermal expansion or disorder, the second one describes the MSRD, the third cumulant or MCRD describes the asymmetry of the pair distribution function, and the fourth one describes the anharmonic contribution to XAFS amplitude. The obtained cumulants describing the high-order expanded DWFs contribute to XAFS spectra of Mo based on Eqs. (1) and (2) shown by good agreement of XAFS FTMs of Mo at 293 K and 573 K calculated using the present theory with experiment [16] (Fig. 5). All the above results for the cumulants and XAFS FTMs provide the accurate information on bcc crystals, i.e., Mo from XAFS experiment.

4. Conclusions

Temperature dependence of high-order expanded Debye-Waller factors and XAFS FTMs of Mo, a bcc crystal, has been studied based on the ACDM derived using the MBPA and the FSNNCA. The calculated results contribute to the valuation of thermodynamic properties and anharmonic effects in XAFS that lead to getting the accurate information on structural and other parameters of bcc crystals taken from XAFS experiment.

The significant discrepancies of the results calculated using the SPP parameters with experiment can be attributed to neglecting the many-body effects in the SPP so that they can be treated by the present theory using the anharmonic effective potential.

The advantage and efficiency of the present theory in XAFS data analysis are illustrated by the good agreement of the numerical results for the cumulants and XAFS FTMs of Mo with experiment. This makes it possible to reproduce the experimental XAFS data of bcc crystals using the present theory.

Acknowledgements

The authors thank Prof. J. J. Rehr and Prof. P. Fornasini for useful comments. This work is funded by the Vietnam National Foundation for Science and Technology Development (NAFOSTED) under grant number: 103.01-2015.10.

References

[1] E. D. Crozier, J. J. Rehr, and R. Ingalls, in X-ray Absorption, edited by D. C. Koningsberger and R. Prins (Wiley, New York, 1988). Chap. 9.
[2] Tranquada J. M. and R. Ingalls R. (1983). Extended x-ray-absorption fine-structure study of anharmonicity of CuBr. Phys. Rev. B 28, 3520.
[3] Stern A., P. Livins, and Zhe Zhang. (1991). Thermal vibration and melting from a local perspective Phys. Rev. B 43, 8850.
[4] Hung N. V., and Frahm R.. (1995). Temperature and Shell Size Dependence of Anharmonicity in EXAFS. Physica B 208 & 209, 91.
[5] Hung N. V., Tien T. S., Duc N. B., Vuong D. Q. (2014). High-order expanded XAFS Debye-Waller factors of hcp crystals based on classical anharmonic correlated Einstein model. Mod. Phys. Lett. B 28, 1450174.
[6] Hung N. V., Duc N. B., Frahm R. R. (2003) A New Anharmonic Factor and EXAFS including Anharmonic Contributions. J. Phys. Soc. Jpn. 72, 1254.
[7] Hung N. V., Tien T. S., Hung L. H., Frahm R. R. (2008). Anharmonic Effective Potential, Local Force Constant and EXAFS of HCP Crystals: Theory and Comparison to Experiment. Int. J. Mod. Phys. B 22, 5155.
[8] Frenkel A. I. and Rehr J. J. (1993). Thermal expansion and x-ray-absorption fine-structure cumulants. Phys. Rev. B 48, 585.
[9] Miyanaga T., Fujikawa T. (1994). Quantum Statistical Approach to Debye-Waller Factor in EXAFS, EELS and ARXPS. III. Application of Debye and Einstein Approximation, J. Phys. Soc. Jpn. 63, 3683.
[10] Hung N. V. and Rehr J. J. (1997). Anharmonic correlated Einstein model Debye-Waller factors. Phys. Rev. B 56, 43.
[11] Daniel M., Pease D. M., Hung N. V., Budnick J. D. (2004). Local force constants of transition metal dopants in a nickel host: Comparison to Mossbauer studies. Phys. Rev. B 68, 134414.
[12] Hung N. V. and Fornasini P. (2007). Anharmonic Effective Potential,Correlation Effects and EXAFS Cumulants Calculated from a Morse Interaction Potential for fcc Metals. J. Phys. Soc. Jpn. 76, 084601.
[13] Hung N. V., L. H. Hung L. H., Tien T. S., Frahm R. R. (2008). Anharmonic Effective Potential, Local Force Constant and EXAFS of HCP Crystals: Theory and Comparison to Experiment. Int. J. Mod. Phys. B 22, 5155.
[14] Hung N. V. (2014). Pressure-Dependent Anharmonic Correlated XAFS Debye-Waller Factors. J. Phys. Soc. Jpn. 83, 024802.
[15] Hung N. V., Thang C. S., Toan N. C., Hieu H. K. (2014). Temperature dependence of Debye-Waller factors of semiconductors. VAC. 101, 63.
[16] V. Pirog I. V. and T. I. Nedoseikina T. I. (2003). Study of pair effective potentials in cubic metals. Physica B 334, 123.
[17] Hung N. V., Hue T. T., Khoa H. D., D. Q. Vuong D. Q. (2016). Anharmonic correlated Debye model high-order expanded interatomic effective potential and Debye-Waller factors of bcc crystals. Physica B, in press.
[18] G. D. Mahan, Many-Particle Physics (Plenum, New York, 1990) 2nd ed.
[19] A. A. Maradudin, Dynamical Properties of Solids, ed. by G. K. Horton and A. A. Maradudin (North Holland, Amsterdam, 1974) Vol. 1, p. 1.
[20] Girifalco L. A. and Weizer W. G. (1959). Application of the Morse Potential Function to Cubic Metals. Phys. Rev. 114, 687.